ACS OMEGA

Open Access

http://pubs.acs.org/journal/acsodf

Article

Biocompatible Native Hyaluronan Nanofibers Fabricated via Aqueous PEO-Assisted Electrospinning and Heat-Quench Process

Komal Raje,[§] Shoya Tanaka,[§] and Satoshi Fujita*

Cite This: *ACS Omega* 2024, 9, 40010−40018

Read Online

ACCESS | Metrics & More | Article Recommendations | Supporting Information

ABSTRACT: Hyaluronan (HA) is widely used in cosmetic and biomedical applications due to its excellent biocompatibility and potential to promote wound healing. Nanofibrous HA, mimicking the extracellular matrix (ECM), is considered promising for therapeutic and cosmetic applications. However, the electrospinning process of HA often necessitates cytotoxic solvents and chemical modifications, compromising its biocompatibility and advantageous properties. In this study, poly(ethylene oxide) (PEO) was added to an aqueous solution of natural HA to improve its spinnability, enabling HA to be electrospun into fibers. The HA was rendered water-insoluble by treatment with an acidic solution, and the amorphized PEO, achieved by heat-quenching, was removed through water washing. This method distinguishes it from previous reports of fibers blended with PEO or other water-soluble polymers. Consequently, the resulting HA gel fibers demonstrated suitability for mesenchymal stem cell adhesion due to the exposure of HA on the fiber surface. Additionally, HA fibers were successfully applied directly onto the skin using a hand-held electrospinning device, indicating the potential for point-of-care and home use applications.

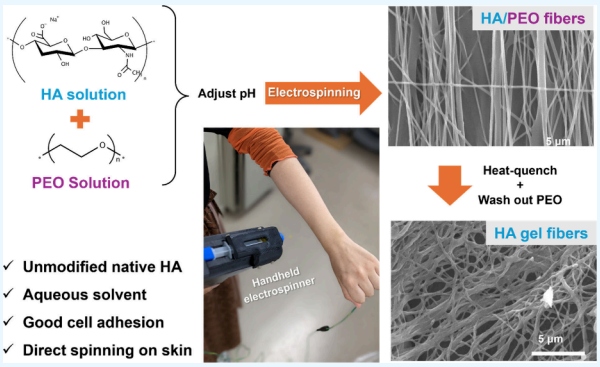

INTRODUCTION

Hyaluronan (HA) is a naturally occurring linear mucopolysaccharide composed of alternating units of *N*-acetyl-D-glucosamine and D-glucuronic acid.[1,2] It is widely found in animal tissue, making it suitable for various biological and medical applications, ranging from cancer treatment to cosmetics.[3−6] Research has extensively focused on HA hydrogels and HA films for use as wound dressings and culture substrates.[7−12] HA hydrogels have been prepared from thiol-modified HA derivatives by oxidation of thiols to promote intermolecular cross-linking.[13] However, this chemical modification has raised safety concerns, particularly regarding its application in medical and cosmetic fields. HA-based composite films have also been explored. For example, the collagen-chitosan-sodium hyaluronate composite film has been utilized for corneal tissue engineering in the rabbit eye.[14] However, fabricating films from HA alone remains challenging. Moreover, as a crucial component of the extracellular matrix (ECM), HA nanofibers fabricated via electrospinning are under investigation for various applications, including tissue engineering, wound therapy, and drug delivery.[15,16] There are still concerns about the use of organic solvents, such as dimethylformamide (DMF) as an electrospinning solvent, particularly in medical and cosmetic applications.

HA nanofibers have also been researched for use as wound dressings since porous nanofibers provide a higher surface area than gels or creams.[17] The porous nanofibrous structure mimics the ECM, while also presenting the potential to deliver bioactive molecules, such as growth factors or therapeutic agents.[18] This study aims to address the existing challenges in HA application, notably the safety concerns associated with using chemically modified HA and the reliance on organic solvents in electrospinning methods. There is a strong desire to develop electrospinning techniques that utilize unmodified, native HA in aqueous solvents, mitigating the safety risks associated with chemical modifications and organic solvents. Here, an electrospinning method for native HA in aqueous condition was explored. We attempted to improve the spinnability by adjusting the pH of the HA solution and by blending it with PEO. Furthermore, the effectiveness of a method combining heat treatment and quenching was demonstrated, which successfully removed PEO by washing after spinning and recovered only HA hydrogel fibers. Additionally, the spinning of HA/PEO fibers directly onto the human body using hand-held electrospinning was investigated due to its potential applications in cosmetics and wound dressing. This approach aims to maintain the biological integrity and safety of HA while leveraging its natural

Received: June 24, 2024
Revised: August 21, 2024
Accepted: September 2, 2024
Published: September 10, 2024

properties for innovative applications in wound dressing and cosmetics.

MATERIALS AND METHODS

Preparation of HA Fibers. HA powder (Kikkoman Biochemifa Company, Japan; MW: 1,800,000−2,000,000) was dissolved in water and stirred overnight to produce solutions with various concentrations, ranging from 0.5% to 2%. PEO (Sigma-Aldrich Japan K.K., Japan; M_v: ∼ 2,000,000) was dissolved in water at concentrations of 0.5%, 0.75% and 1%. The unadjusted HA/PEO solution had a pH of 8.5. Both were mixed to prepare the HA/PEO solution, which was adjusted to an acidic pH using HCl. The pH 4-adjusted HA/PEO solutions were used for electrospinning.

Electrospinning was performed on a rotating drum collector using NANON-01B (MECC Co. Ltd., Japan) equipped with a 23G needle. The parameters were set as follows: flow rate of 0.2−1.0 mL/h, electric field of 1.0−3.0 kV/cm, and linear velocity of 20.9 m/s. The HA/PEO fibers were collected on either cover glass or aluminum foil attached to the collector.

Electrospun fibers from the 1.5% HA/1.0% PEO solution, hereafter referred to as HA/PEO fibers, were used for all subsequent experiments. HA/PEO fibers were heated to 100 °C for 30 min in an oven and then quenched to 0 °C using a dry bath. The sample was subsequently immersed in a 0.2 M acetic acid aqueous solution for 10 min. The prepared fibers were washed with RO water to remove PEO, resulting in HA gel fibers (Scheme 1). To produce HA and PEO films, 3% HA solution and 2% PEO solution, respectively, were spread on separate 35 mm dishes and dried at room temperature for 3 days.

Scheme 1. Fabrication Process of HA Gel Fibers (Blue Lines Indicate PEO)

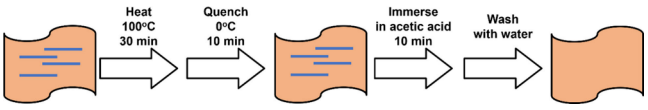

Hand-Held Electrospinning. A solution with a pH of 4, composed of 1.5% HA and 1.0% PEO containing 0.1% vitamin B2, was used for direct electrospinning onto skin using a hand-held device supplied by MECC Co. Ltd. Japan. The device specifications included a 23G needle and an electric field of 1 kV/cm. The HA/PEO solutions were electrospun at various flow rates, ranging from 1 to 3.5 mL/h, to evaluate the spinnability of the solutions.

Characterization of HA/PEO Solutions. The dynamic viscoelasticity of the HA/PEO solutions was measured using a rheometer (MCR302/F, Anton Paar GmbH, Austria). For the experiments, 1 mL of the solution was applied onto a cone−plate rheometer (CP25) kept at 25 °C. Strain dependence measurements were performed at an angular velocity of 1 rad/s. Frequency dependence was measured at 0.5% strain for the HA/PEO solution and at 1% strain for the individual HA and PEO solutions.

The zeta potential of the HA/PEO solutions was measured using a Nanoparticle Analyzer SZ-100 (HORIBA Ltd., Japan) with an electrode cell (carbon 6 mm) at one-tenth the concentration used for electrospinning.

Characterization of Fibers. For SEM observation, the HA/PEO fibers and HA gel fibers were dehydrated in ethanol (EtOH) by stepwise increments of the EtOH concentration from 50% to 100%, followed by replacement with t-butyl alcohol and refrigeration, as per standard protocol for preparation of hydrogel samples for SEM observation.[19,20] On complete freezing, the samples were lyophilized using ES-2030 (Hitachi, Japan) at 26 Pa and −10 °C for 2 h. The samples were then coated with osmium (MSP-1S, Vacuum Device, Japan) before observation in desktop SEM (JEOL, JSM6390FMM) at an accelerating voltage of 15 kV. Fiber diameters were measured from the SEM images using ImageJ.[21]

Polarized light microscopy observation (Olympus BX53, Olympus Optical Co. Ltd., Japan) was performed to investigate the crystalline state of PEO in the HA/PEO fibers. Images were taken at angles of 0° and 45°, and the 45° images were rotated using ImageJ. Alcian blue stain was added to the washed HA gel fibers and soaked for 10 min for visualization of HA.

Differential scanning calorimetry (DSC) was performed using a thermal analyzer (DSC-60, Shimadzu Corp., Japan) between the temperature range: 30−120 °C at a heating rate of 5 °C/min, using an empty aluminum pan as a reference. The degree of crystallinity (X′) was calculated using the following eq 1:

$$X' = \frac{\Delta H_m}{\Delta H_0(1 - C_{CNF})} \times 100 \quad (1)$$

Wide-angle X-ray diffraction (WAXD) was performed using an X-ray diffractometer (Ultima IV, Rigaku Corp., Japan) at a sample−detector distance of 93 mm, with q range of approximately 4−30 nm^{-1} at 25 °C. The samples were set parallel and perpendicular, and measurements were taken, respectively. Attenuated total reflectance-Fourier transform infrared (ATR-FTIR) spectrometry was performed on Thermo-Nicolet 6700 (Thermo Fisher Scientific, USA) with 64 integrations across 400−4,000 cm^{-1} at 45° angle of incidence with a resolution of 4 cm^{-1}. Spectra measured without sample were used as background.

Cell Culture. Dulbecco's modified Eagle's medium (DMEM) supplemented with 10% fetal bovine serum (FBS) and 1% Penicillin-Streptomycin solution, hereafter referred to as media, was used in cell culture experiments. HA gel fibers were placed in a 35 mm tissue culture dish and stained for about 3 min with Alcian blue solution sterilized using a sterile filter (Millex-GP Filter, 0.22 μm, PES 33 mm). The fibers were rinsed with phosphate-buffered saline (PBS) until background was removed. Next, 2 mL of media was added, aspirated and fresh 2 mL of media was added. Human bone marrow mesenchymal stem cells (hBM-MSCs, Takara Bio, Japan) or HEK293 cells were seeded onto the fibers at 5×10^4 cells/ml. Cell culture was performed at 37 °C under 5% CO_2 for 7 days.

Cells cultured on HA fibers for 7 days were stained and observed using a fluorescence microscope (Olympus IX-81, Olympus Optical Co. Ltd., Japan). To prepare the cells for staining, media was aspirated, and the cell-laden fibers were washed twice with 1 mL of PBS. Next, the fibers were fixed using 0.5 mL of 4% paraformaldehyde/PBS solution incubated at 37 °C for 15 min. The specimens were then treated with 2 mL of 0.005% Tween 20/PBS and Blocking One (Nacalai, Japan). A staining solution of 2 mL of Blocking One, 2 μL of Alexa488-Phalloidin was added, and the specimens were incubated at room temperature for 2 h. Finally, the specimens

https://doi.org/10.1021/acsomega.4c05851
ACS Omega 2024, 9, 40010−40018

were washed twice with PBS and observed using a fluorescence microscope while still in PBS.

RESULTS

Characterization of HA/PEO Electrospinning Solutions. The dissociation state of HA side chains influences the viscosity and resultant spinnability of the solution. The viscoelastic properties of electrospinning solutions across a range of pH values were examined (Figure S1). The initial pH of 1.5% HA/1% poly(ethylene oxide) (PEO) aqueous solution was 8.5, adjusted to between 3 and 6 using HCl. The dependency of the viscoelastic properties on angular frequency using a rheometer was carried out. Lowering the pH resulted in a reduced complex viscosity. At lower pH values, the slope of the viscosity-angular frequency graph decreased, indicating less change in viscosity with alterations in angular frequency, thereby reducing the thixotropic properties of the HA/PEO solution. Both the loss modulus (G'') and the storage modulus (G') declined at lower pH. In the low-frequency range, G'' exceeded G' across all pH levels, indicating sol-like behavior. As the frequency increased, G' became dominant, with the intersection of G' and G'' signifying gelation of the solution. When plotting the viscoelastic properties of the solution at different pH levels, the gelation point shifted toward higher frequencies as pH decreases, whereas the complex viscosity at the gel point decreases with lower pH (Figure 1).

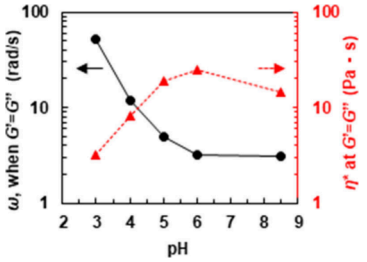

Figure 1. Rheological properties of HA/PEO solutions at different pH values. The graph displays the angular frequency (ω, when $G' = G''$) as a function of pH (black line with circles) and the complex viscosity (η^*, when $G'' = G'$) plotted against pH (red dashed line with triangles).

The zeta potentials for the 0.15% HA and the 0.15% HA/0.1% PEO solutions were measured (Supporting Information Figure S2). The zeta potential of PEO was −31.4 mV, and the HA/PEO solution showed a positive shift in zeta potential as the pH decreased. Similar results were observed in solutions containing only HA. These results suggest that at low pH, the carboxy groups of the HA chain remain uncharged, reducing electrostatic repulsion within the HA molecule and facilitating its interaction with PEO. Conversely, at higher pH, increased electrostatic repulsion between HA units may lead to reduced molecular flexibility, thereby increasing the solution's viscosity. As the solution undergoes high strain during ejection in the electrospinning, maintaining a sol state even at high frequencies is advantageous. Therefore, lower pH solutions are more suitable for injection during electrospinning. However, if the solution's viscosity is too low, spinnability will decrease, suggesting that an optimal pH range for electrospinning exists.

Spinnability of HA/PEO Solution and Fiber Morphology. When the HA concentration was held constant and the PEO concentration was varied, both the number of fibers and their spinnability decreased with reduced PEO concentration. Changes in HA concentration did not affect spinnability when the PEO concentration was maintained. At 1% HA/0.5% PEO, beaded fibers were obtained. Given the sparsity of the obtained fibers, the PEO concentration was increased. Increasing the HA concentration to 2.0% resulted in a loss of uniformity and an increase in fiber diameter, along with reduced spinnability. Based on these findings, the optimal concentration was determined to be 1.5% HA/1.0% PEO.

pH conditions were investigated for the 1.5% HA/1.0% PEO solutions by adjusting the pH from 3 to 6 using HCl. The electrospinning voltage and flow rate were optimized, and a cover glass was mounted on the grounded collector to collect fibers. Figure 2 shows representative SEM images of fibers, and

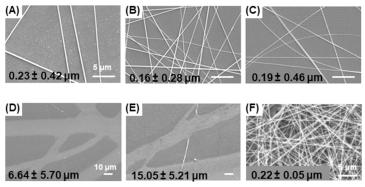

Figure 2. SEM images and averaged fiber diameter of nanofibers obtained from 1.5% HA/1.0% PEO solutions at various pH and a 2% PEO control. (A) pH 3, (B) pH 4, (C) pH 5, (D) pH 6, (E) pH 8.5, and (F) 2% PEO.

Figure S3 shows the distribution of fiber diameters. At pH 3 to 5, thin and uniform fibers were obtained (Figure 2A–C). Among them, the largest number of fibers was obtained at pH 4, where good spinnability was observed across various spinning conditions. Regarding fiber diameter, fibers from pH 4 solution were the thinnest and most uniform (Figure S3). On the other hand, at pH 6 and at unadjusted pH, nanosized fibers could not be achieved; only thick fibers were formed, resulting in a significant decrease in spinnability (Figure 2D,E). Based on this result, the 1.5% HA/1.0% PEO solution with pH 4 was selected for further experiments.

Crystallinity of PEO in HA/PEO Fibers. To further investigate the crystalline state of PEO within the HA/PEO fibers prepared at various pH, WAXD and DSC analyses were performed. Peaks characteristic of PEO crystals, specifically the 120 and 112 planes 20, were identified in HA/PEO fibers (Figure 3A). Notably, the intensity of these peaks decreased as the pH of the preparation decreased. DSC results complemented these findings, revealing that the addition of HA shifted the melting point of PEO to a lower temperature. Additionally, there was a reduction in both the enthalpy of fusion and the degree of crystallinity as the pH was lowered (Figure 3B). These results, aligned with the WAXD findings, indicate that the PEO crystals within the HA/PEO fibers were suppressed due to entanglement with the HA chains, particularly at lower pH. This suggests a significant interaction between HA and PEO, influenced by the acidity of the environment, which impacts the crystalline structure and thermal properties of PEO within the composite fibers.

Morphology of HA Fibers. To confirm whether the washed HA fibers maintained their fiber structure, SEM observation was performed on the HA/PEO fiber mat before and after washing (Figure 4A,B). The fiber structure was intact in the sheet before washing. The average diameters of the HA/PEO fibers before and after washing were 150 ± 20 nm and

https://doi.org/10.1021/acsomega.4c05851
ACS Omega 2024, 9, 40010−40018

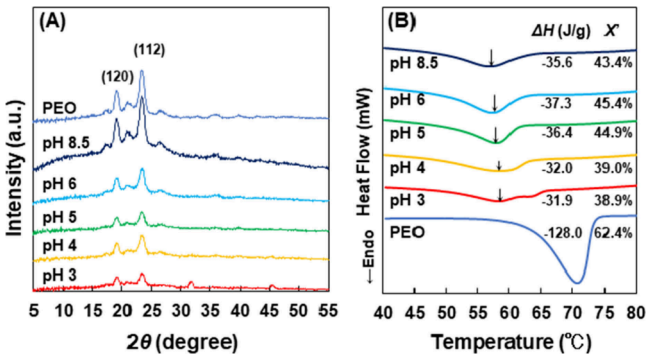

Figure 3. Characterization of fibers electrospun from 1.5% HA/1% PEO solutions at different pH. (A) WAXD patterns of HA/PEO fibers. Scattering angles, 5−55°; scan rate, 0.5°/min. (B) DSC thermograms of HA/PEO fibers showing the enthalpy of melting peaks derived from PEO. Heating rate, 5 °C/min; temperature range, 30−120 °C. Graphs include PEO fibers for comparison.

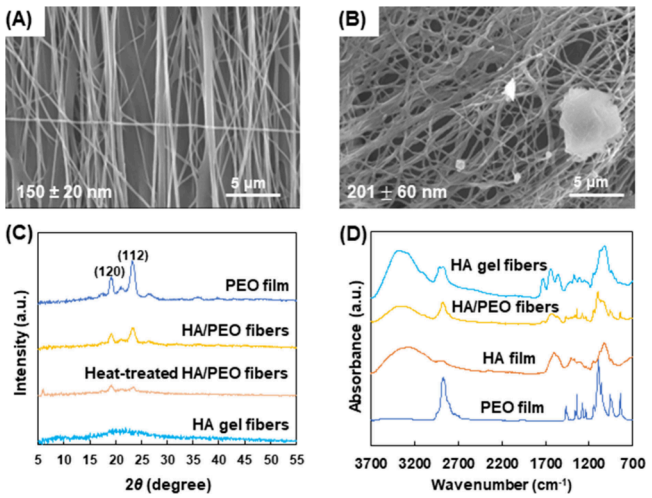

Figure 4. Effect of washing treatment on HA/PEO nanofiber mats. (A) SEM image of the nanofiber mat before washing and (B) postwashing. Bar = 5 μm. (C) WAXD patterns for fibers before and after washing. Scattering angles, 5−55°; scan rate, 0.5°/min. (D) ATR-FTIR spectra.

201 ± 60 nm, respectively, indicating an increase of approximately 50 nm. Additionally, the oriented structure of the fiber mat collapsed, and adjacent fibers adhered together. This would be due to repeated washing operations and slight damage of the fibers. Contact angle measurements were also attempted, but because of the hydrophilicity of HA and PEO, the water droplets spread completely, preventing accurate angle measurements.

WAXD. To determine the crystalline state and removal of PEO before and after washing, WAXD measurements were taken on as-spun HA/PEO fibers, HA/PEO fibers after heating and quenching, and HA fibers postwashing (Figure 4C). Peaks attributed to PEO crystals ((120) and (112) planes) were observed in as-spun HA/PEO fibers. The peak intensities of the (120) and (112) planes in HA/PEO fibers subjected to heating and quenching were reduced by about half, indicating that most PEO crystals became amorphous due to the heating and quenching process. In HA gel fibers after washing, the peaks from PEO crystals, specifically (120) and (112) planes, completely disappeared, indicating that PEO was entirely removed from the HA/PEO fibers during the washing operation.

ATR-FTIR. To investigate the removal of PEO in detail, heat-quenched HA/PEO fibers and HA gel fibers were analyzed using ATR-FTIR, compared with PEO cast film and HA cast film (Figure 4D). The ATR-FTIR analysis revealed characteristic peaks of PEO at 2869 cm^{-1} (CH_2 stretching vibration) and 1080 cm^{-1} (C−O−C stretching vibration) 20 in PEO powder, HA/PEO fibers and heat-quenched HA/PEO fibers. No PEO-derived peak at 1080 cm^{-1} was observed in the HA gel fibers, suggesting the removal of PEO during the washing process. Additionally, peaks at 1670 cm^{-1} (amide group, C═O stretching vibration), 1550 cm^{-1} (N−H bending vibration), and at 1430 cm^{-1} (N−H stretching vibration)[17] in HA/PEO fibers, heat-quenched HA/PEO fibers and HA cast film. The presence of HA-derived peaks in HA gel fibers confirmed that HA was not dissolved or removed by the washing operation, showing that HA gel fibers are water-insoluble.

Alcian Blue Staining. To confirm the presence of HA in the HA gel fibers obtained after the washing operation, Alcian blue staining was performed. Alcian blue, a phthalocyanine-based basic dye, forms an ionic bond with the acidic groups, including carboxy group, present in HA but does not interact with PEO. It was observed that entire fiber mat and each individual fibers exhibited a blue color due to Alcian blue (Figure 5). The fiber structure was also maintained through

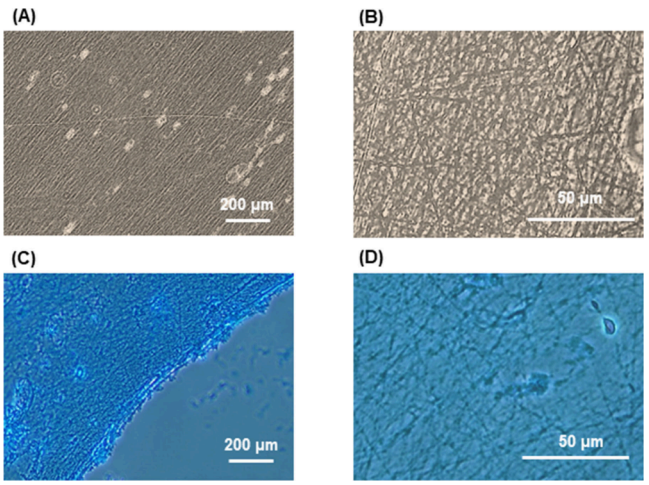

Figure 5. Bright-field microscopy images of HA/PEO fibers. (A, B) As-spun HA/PEO fibers showing their initial morphology. (C, D) Fibers after washing and Alcian blue staining.

the washing treatment. This indicates that HA did not dissolve in water during the washing procedure and confirms the presence of HA in the washed fibers.

Polarized Light Microscopy. The birefringence of PEO crystals can be exploited to confirm the existence of PEO crystals in a sample. PEO fibers, HA cast films, HA/PEO fibers, and HA gel fibers were observed using a polarizing microscope (Figure 6). In the fiber mat containing only PEO, birefringence was observed throughout the sample, confirming the presence of PEO throughout the fiber (Figure 6A,B). On the other hand, since HA is amorphous and no birefringence is observed, no birefringence was observed in the HA cast film (Figure 6C,D). In the HA/PEO fiber, birefringence was observed throughout the fiber, indicating that PEO was well-distributed

https://doi.org/10.1021/acsomega.4c05851
ACS Omega 2024, 9, 40010−40018

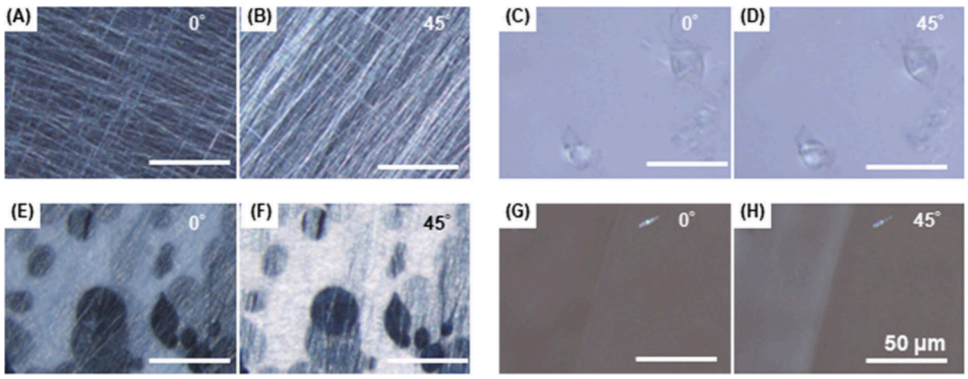

Figure 6. Polarizing microscopic images demonstrating the effects of orientation and washing treatment. (A, B) PEO fibers at stage angles of 0° and 45°, respectively, displaying distinct fiber alignments. (C, D) HA film, showing no birefringence. (E, F) As-spun HA/PEO fibers before washing. (G, H) HA gel fibers after washing, also showing no birefringence. Scale bars = 50 μm.

throughout the fiber (Figure 6E,F). No birefringence was observed in the HA gel fibers (Figure 6G.H), likely due to the removal of PEO by washing the HA/PEO fiber.

To summarize the results above, WAXD and ATR-FTIR analyses confirm the complete removal of PEO from HA gel fibers, as evidenced by the absence of PEO-derived peaks corresponding to the (120) and (112) crystal planes.[22,23] This is further supported by Alcian blue staining, which confirms that no PEO remains to inhibit the interaction of HA molecules with other substances. Additionally, the polarized light microscopy observed in the washed HA gel fibers (Figure 6G,H) suggests that the fibers folding over each other during cleaning rather than indicating the presence of residual PEO. The method to produce insolubilized HA gel fibers from HA/PEO fibers exploits the characteristics of the crystalline region of PEO and the carboxy group of HA, avoiding the need for potentially harmful cross-linking reagents or organic solvents. The established HA/PEO fiber cleaning and insolubilization process maintained the fiber structure even after washing, removed PEO, and demonstrated that the remaining fiber structure is indeed HA.

Cell Culture. To investigate the biocompatibility of HA gel fibers and the initial adhesion of cells, human embryonic kidney cells 293 (HEK293) and human bone marrow mesenchymal stem cells (hBM-MSCs) were seeded on HA gel fibers and cultured for 7 days (Figure 7). It was observed that while HEK293 cells adhered better to the dish surface than to the HA gel fibers, hBM-MSCs stretched on the fibers. These results indicate that the washed HA gel fibers are suitable for the initial adhesion of hBM-MSCs. This adhesion is likely due to the presence of the HA receptor CD44, a type I transmembrane glycoprotein that mediates cell−cell interactions through its affinity for HA.[24] Since HEK293 cells do not express CD44, they did not adhere to the HA gel fibers, showing the selectivity of the HA gel fibers for CD44-positive cells.

Direct Spraying onto Skin with Hand-Held Electrospinning. Nanofibers made from hand-held electrospinning of HA, an ECM component, were investigated for potential use as wound dressings and cosmetics. HA/PEO nanofibers were directly electrospun onto the skin using a prototype hand-held electrospinning machine (Figure 8A). A 1.5% HA/1.0% PEO solution supplemented with 0.1% vitamin B2 (pH 4) was also spun onto the skin, and its presence was confirmed using black light. Vitamin B2, also known as riboflavin, is water-soluble and fluoresces yellow under UV light.[25]

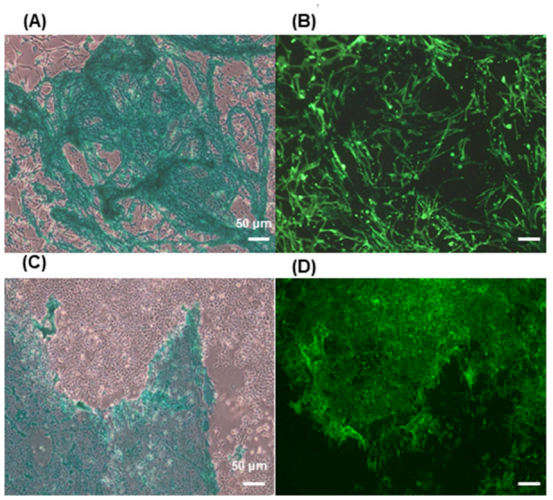

Figure 7. Microscopy images of cell cultures on HA gel fibers after 7 days. (A, B) hBM-MSC and (C, D) HEK293 cells. (A, C) Alcian blue staining of HA gel fibers. (B, D) Same fields of immunofluorescence images displaying actin fibers stained Alexa488-Phalloidin (green). Scale bars = 50 μm.

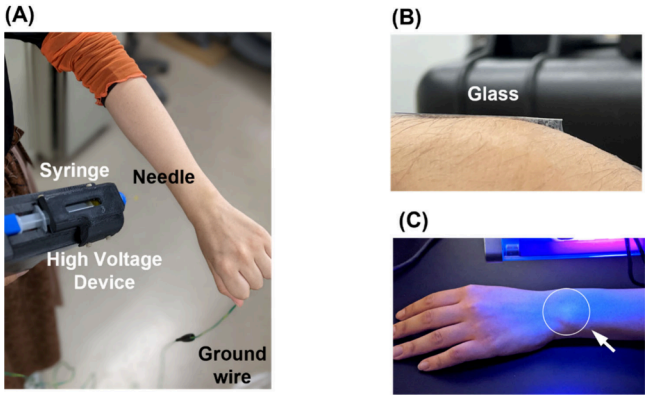

Figure 8. Hand-held electrospinning of HA/PEO fibers: (A) Electrospinning directly onto an arm. (B) Fibers deposited on a cover glass mounted on human skin. (C) HA/PEO fiber solution containing vitamin B2 sprayed and visualized under black light, with yellow areas indicating fiber deposition (arrow).

In hand-held electrospinning, a circuit is formed by holding the main device in one hand and the ground wire in the other (Figure 8A). Thus, fibers are spun onto the skin in the same

https://doi.org/10.1021/acsomega.4c05851
ACS Omega 2024, 9, 40010−40018

manner as in a normal electrospinning device. To observe the fiber morphology created using a microscope, a coverslip was placed on the skin and spun (Figure 8B). The formation of a fibrous membrane in the gap between the cover glass and the skin can be noted with the naked eye. Furthermore, when spinning with a solution containing 0.1% vitamin B2, yellow fluorescence was emitted upon irradiation with black light (Figure 8C), indicating that fibers were indeed spun onto the skin. At low voltage and flow rate, spinning did not occur. Fibers were formed when the voltage and flow rate were increased to 1.5 kV/cm and 2.5 mL/h, and the most fibers were observed at 20 kV/cm and 2.5 mL/h. Under all conditions, bead-like fibers were formed. These results showed that HA/PEO fibers that could be created by conventional electrospinning setup can be spun onto the skin by hand-held electrospinning using the same solution.

DISCUSSION

Electrospinning of Native HA. One challenge with using HA as a cell scaffolding material is its solubility in body fluids and culture media. To address this, research has focused on creating water-insoluble HA fibers through cross-linking. Nanofiber-like scaffolds have been developed from electrospinning a cross-linked thiolated HA derivative, which maintained their fibrous structure during cell culture.[15] Similarly, HA cross-linked with adipic acid dihydrazide and electrospun into nanofiber mats showed good water resistance and maintained mechanical stability for up to 2 weeks,[26] indicating their potential for cell culture applications. However, native HA is highly desired because of safety concerns.

During the electrospinning of native HA, a charged biopolymer, it forms a highly viscoelastic solution even at low concentrations due to intramolecular electrostatic interactions and counterions, resulting in poor spinnability without specialized solvents.[27,28] Studies have used organic solvents to adjust the conductivity, surface tension, and viscosity of the solution, thus improving spinnability.[29,30] Electrospun HA nanofibers have been fabricated using mixed solvents of water, DMF, and formic acid.[31] Formic acid disrupts the rigid helix structure of HA, promoting new hydrogen bonds and better chain entanglements. Its partial ionization also enhances conductivity and jet length, further improving spinnability. Additionally, a mix of aqueous ammonium hydroxide and DMF has been used to further improve spinnability and reduce fiber diameters.[28] However, the use of corrosive acids and organic solvents raises safety concerns for biological applications, such as direct human contact or as scaffolds in cell culture.

Fabricating native HA nanofibers in aqueous conditions without using harmful solvents and chemical cross-linking has been challenging for medical applications. The difficulty arises because the dissociation of carboxy groups leads to negative charge repulsion, and high water-absorption of HA increases the solution viscosity, complicating electrospinning.[32] As demonstrated in our previous studies,[36,37] using other water-soluble polymers as guide polymers for electrospinning is particularly effective when dealing with materials that are difficult to fibrillate. We have previously implemented a method to improve spinnability of other materials by adding PEO to the electrospinning solution, and thus, considered PEO for this study as well.[33,34] There have been attempts to blend HA with water-soluble polymers such as PEO and PVA. Aqueous blends of poly(vinyl alcohol) (PVA) or PEO with HA resulted in beaded nanofibers.[33] Electrospinning HA with low-molecular-weight PEO produced HA fibers decorated with PEO beads, which reduced the electrostatic repulsion of HA and improved chain entanglement without contributing to fiber structure.[35] In contrast, blending HA with high-molecular-weight PEO formed fibers where the diameter is restricted by the large size of PEO.[36] However, these fibers were too sparse for scaffold use. Adding cationic chitosan (CS) could mitigate electrostatic repulsion among anionic HA molecules, forming coacervates that enable longer fibers.[32,37] Notably, HA alone did not adequately support cell attachment.[36]

In this study, HA/PEO fibers were fabricated from a low-concentration PEO solution and a pH-adjusted HA solution. It is known that excessively high solution viscosity decreases spinnability;[38] however, lowering the pH reduced the viscosity of the HA solution, as shown in Figures 1 and S1, thereby improving its spinnability. By mixing the HA and PEO solutions, the spinnability of HA/PEO nanofibers was successfully enhanced without using organic solvents. While several studies have employed HA/PEO electrospinning for biomaterial applications, the added polymers are generally not removed, resulting in composite fibers. This is supported by the higher concentration of lower molecular weight PEO employed in the electrospinning solution,[39,40] and a lack of washing process. HA/PEO composite nanofibers have demonstrated potential as carriers of hydrophilic antibiotics for targeting microbes[39] as well as natural active components for enhanced wound healing.[40]

Here, upon removing PEO through heating followed by water washing, fibers predominantly composed of native HA were obtained. FTIR observations showed that while PEO was largely removed, some remained, as indicated by a characteristic peak of PEO at 2869 cm^{-1} after the washing treatment. However, polarized light microscopy showed that little PEO remains in the crystallized state; the residual PEO is amorphous, as no crystallinity is observed. This amorphous PEO does not contribute to physical cross-linking via microcrystals, not significantly impacting the mechanical properties of the composite material. Furthermore, PEO is a widely used and safe polymer in pharmaceuticals and cosmetics, posing no toxicity concerns when used in biomedical applications.[41−43] Therefore, the presence of residual PEO in the composite does not compromise safety.

The suppression of HA dissociation under acidic conditions makes HA less soluble and promotes hydrogen bond formation between HA molecules.[44,45] When returned to neutral pH, the nanofibers remain stable due to intra- and intermolecular hydrogen bonds, which is considered the primary mechanism of hydrogel formation. Since PEO lacks electrostatic interaction sites with HA, physical interactions beyond molecular entanglement are improbable. However, it is known that proteins can form insoluble complexes with HA through coacervation.[46,47] As cell culture media contain serum-derived proteins, this complex formation may also stabilize HA in the culture medium.

Cell Culture Study. The biocompatibility of the HA gel fibers was confirmed using two different cell cultures; HEK293 and hBM-MSCs. While HEK293 cells showed a preference for the tissue culture dish surface over the HA gel fibers, hBM-MSCs stretched on the fibers. The selective adhesion is likely driven by the presence of CD44, an HA receptor, on hBM-MSCs and its absence in HEK293 cells. This further

https://doi.org/10.1021/acsomega.4c05851
ACS Omega 2024, 9, 40010−40018

demonstrates that HA is present in its native form. HA, an abundant extracellular matrix component in brain tissue, composes the anisotropic structure of HA fibers. Therefore, the HA fibers produced in this experiment could be useful as culture substrates that mimic the pericellular microenvironment in the brain.

Availability of Hand-held Electrospinning. Hand-held electrospinning devices, which directly deposit nanofibrous mats on surfaces, have recently emerged as promising alternatives to conventional equipment, particularly for wound dressing and cosmetic applications.[48−51] These devices offer portability, ease of use without a power source, and low cost. Their portability makes them suitable for emergency clinical settings or remote areas where conventional electrospinning setups are impractical. Additionally, these devices are easy to use at home and can produce nanofibers with quality equivalent to those produced by benchtop ones.[52]

Hand-held electrospinning has been reported to directly electrospin poly(vinyl butyral) (PVB) nanofibers onto primary human dermal fibroblast cells with EtOH/water solvents, reducing cytotoxicity and maintaining cell viability.[53] It has also been utilized for spinning dyed polyacrylonitrile fibers[54] and polycaprolactone fibers with Ag-decorated mesoporous silica nanoparticles.[49] These fiber mats have demonstrated potential as broad-spectrum antibacterial wound dressings with accelerated healing. Another advancement includes a battery-powered portable electrospinning device using AAA batteries and a high-voltage converter, capable of applying voltages up to 10 kV to the needle without using a standard high-voltage power supply.[55] Current research on hand-held electrospinning materials often involves organic solvents and synthetic polymers that are potentially harmful to the human body.[55−57] To avoid adverse effects from solvents, some electrospinning devices utilize melt electrospinning,[58,59] although the high temperatures required to melt the polymers might damage tissue further.

Most hand-held electrospun dressings previously reported use synthetic and nonbiodegradable polymers. HA, as a safe biomaterial, has broad potential in cosmetics and medical products. HA-based wound dressings produced using hand-held devices could be especially beneficial, potentially opening a new market for custom-made dressings tailored to individual patients.

In our study, nanofibers containing up to 60% HA were successfully electrospun onto the skin using hand-held electrospinning. This marks the first successful hand-held electrospinning of native HA using aqueous solvents, suggesting potential applications in wound dressing or cosmetics. Unlike conventional benchtop electrospinning, hand-held electrospinning is more susceptible to environmental factors such as weather, humidity, and temperature, which can sometimes prevent electrospinning. However, hand-held electrospinning offers flexibility in adjusting parameters such as the needle-collector distance and the needle orientation, facilitating easy adjustment of conditions, but potentially destabilizing the HA/PEO solution. As PEO-assisted HA electrospinning employing the heat-quench method cannot currently be performed on the skin, further improvements are needed to address this issue. Therefore, developing a system that allows for the tuning of spinning conditions in response to the environment remains a significant challenge.

CONCLUSIONS

In this study, HA gel fibers were successfully electrospun using a pH-adjusted HA/PEO solution. Adjusting the pH altered the physical properties of the solution, improving its spinnability and enabling the production of water-insoluble HA gel fibers. Cell culture experiments demonstrated the biocompatibility of these fibers, promoting selective cell adhesion.

Previously, spinning HA gel fibers required organic solvents or chemically modified HA. This study, however, achieved the fabrication of thin, uniform fibers using native HA in an aqueous solvent. The HA gel fibers contained minimal amounts of PEO, safe for use in medicines and cosmetics, suggesting they are compatible for human skin. The newly established washing procedure involving the heat-quench treatment allows the fabrication of fibers composed mainly of HA, a natural polymer.

Additionally, hand-held electrospinning of the aqueous HA/PEO solution was also demonstrated. This advancement in spinning native natural polymers using aqueous solvents holds potential for developing cell culture scaffolds, wound dressings, and cosmetics.

ASSOCIATED CONTENT

Supporting Information

The Supporting Information is available free of charge at https://pubs.acs.org/doi/10.1021/acsomega.4c05851.

(Figure S1) rheological properties; (Figure S2) ζ potentials; (Figure S3) fiber diameter distribution analysis (PDF)

AUTHOR INFORMATION

Corresponding Author

Satoshi Fujita − *Department of Frontier Fiber Technology and Sciences, University of Fukui, Fukui 910-8507, Japan; Life Science Innovation Center, University of Fukui, Fukui 910-8507, Japan;* orcid.org/0000-0003-1438-6402; Phone: +81-776-27-9969; Email: fujitas@u-fukui.ac.jp; Fax: +81-776-27-9969

Authors

Komal Raje − *Department of Frontier Fiber Technology and Sciences, University of Fukui, Fukui 910-8507, Japan;* orcid.org/0000-0002-8131-8146

Shoya Tanaka − *Department of Frontier Fiber Technology and Sciences, University of Fukui, Fukui 910-8507, Japan*

Complete contact information is available at: https://pubs.acs.org/10.1021/acsomega.4c05851

Author Contributions

The manuscript was written through contributions of all authors. All authors have given approval to the final version of the manuscript. K.R.: Data curation and writing−original draft. S.T.: Data curation, methodology, writing−original draft, and visualization. S.F.: Conceptualization, methodology, investigation, validation, writing−original draft, reviewing, and editing.

Author Contributions

[§]K.R. and S.T. contributed equally to this work.

Notes

The authors declare no competing financial interest.

https://doi.org/10.1021/acsomega.4c05851
ACS Omega 2024, 9, 40010−40018

■ ACKNOWLEDGMENTS

The handheld electrospinner was provided by MECC Co. Ltd. (Fukuoka, Japan).

■ ABBREVIATIONS

ATR-FTIR, attenuated total reflectance-Fourier transform infrared; CS, chitosan; DMEM, Dulbecco's modified Eagle's medium; DMF, *N*,*N*-dimethylformamide; DSC, differential scanning calorimetry; ECM, extracellular matrix; EtOH, ethanol; FBS, fetal bovine serum; HA, hyaluronan; hBM-MSCs, human bone marrow mesenchymal stem cells; HEK293, human embryonic kidney 293; PBS, phosphate-buffered saline; PEO, poly(ethylene oxide); PVA, poly(vinyl alcohol); SEM, scanning electron microscopy; WAXD, wide-angle X-ray diffraction

■ REFERENCES

(1) Weissmann, B.; Meyer, K. The Structure of Hyalobiuronic Acid and of Hyaluronic Acid from Umbilical Cord. *J. Am. Chem. Soc.* **1954**, *76* (7), 1753−1757.
(2) Kaye, M. A.; Stacey, M. Chemistry of tissues; methylation studies on hyaluronic acid. *Biochem. J.* **1951**, *48* (2), 249−255.
(3) Yasin, A.; Ren, Y.; Li, J.; Sheng, Y.; Cao, C.; Zhang, K. Advances in Hyaluronic Acid for Biomedical Applications. *Front. Bioeng. Biotechnol.* **2022**, *10*, No. 910290.
(4) Cho, H.-J. Recent progresses in the development of hyaluronic acid-based nanosystems for tumor-targeted drug delivery and cancer imaging. *J. Pharm. Investig.* **2020**, *50* (2), 115−129.
(5) Gomes, C.; Silva, A. C.; Marques, A. C.; Sousa Lobo, J.; Amaral, M. H. Biotechnology Applied to Cosmetics and Aesthetic Medicines. *Cosmetics* **2020**, *7* (2), 33.
(6) Huang, G.; Huang, H. Hyaluronic acid-based biopharmaceutical delivery and tumor-targeted drug delivery system. *J. Controlled Release* **2018**, *278*, 122−126.
(7) Bazmandeh, A. Z.; Mirzaei, E.; Fadaie, M.; Shirian, S.; Ghasemi, Y. Dual spinneret electrospun nanofibrous/gel structure of chitosan-gelatin/chitosan-hyaluronic acid as a wound dressing: In-vitro and in-vivo studies. *Int. J. Biol. Macromol.* **2020**, *162*, 359−373.
(8) Chanda, A.; Adhikari, J.; Ghosh, A.; Chowdhury, S. R.; Thomas, S.; Datta, P.; Saha, P. Electrospun chitosan/polycaprolactone-hyaluronic acid bilayered scaffold for potential wound healing applications. *Int. J. Biol. Macromol.* **2018**, *116*, 774−785.
(9) Voigt, J.; Driver, V. R. Hyaluronic acid derivatives and their healing effect on burns, epithelial surgical wounds, and chronic wounds: a systematic review and meta-analysis of randomized controlled trials. *Wound Repair Regen.* **2012**, *20* (3), 317−331.
(10) Arulmoli, J.; Wright, H. J.; Phan, D. T. T.; Sheth, U.; Que, R. A.; Botten, G. A.; Keating, M.; Botvinick, E. L.; Pathak, M. M.; Zarembinski, T. I.; Yanni, D. S.; Razorenova, O. V.; Hughes, C. C. W.; Flanagan, L. A. Combination scaffolds of salmon fibrin, hyaluronic acid, and laminin for human neural stem cell and vascular tissue engineering. *Acta Biomater.* **2016**, *43*, 122−138.
(11) Zamboni, F.; Keays, M.; Hayes, S.; Albadarin, A. B.; Walker, G. M.; Kiely, P. A.; Collins, M. N. Enhanced cell viability in hyaluronic acid coated poly(lactic-co-glycolic acid) porous scaffolds within microfluidic channels. *Int. J. Pharm.* **2017**, *532* (1), 595−602.
(12) Zhang, K.; Shi, Z.; Zhou, J.; Xing, Q.; Ma, S.; Li, Q.; Zhang, Y.; Yao, M.; Wang, X.; Li, Q.; et al. Potential application of an injectable hydrogel scaffold loaded with mesenchymal stem cells for treating traumatic brain injury. *J. Mater. Chem. B* **2018**, *6* (19), 2982−2992.
(13) Shu, X. Z.; Liu, Y.; Luo, Y.; Roberts, M. C.; Prestwich, G. D. Disulfide cross-linked hyaluronan hydrogels. *Biomacromolecules* **2002**, *3* (6), 1304−1311.
(14) Chen, J.; Li, Q.; Xu, J.; Huang, Y.; Ding, Y.; Deng, H.; Zhao, S.; Chen, R. Study on biocompatibility of complexes of collagen-chitosan-sodium hyaluronate and cornea. *Artif. Organs* **2005**, *29* (2), 104−113.
(15) Ji, Y.; Ghosh, K.; Li, B.; Sokolov, J. C.; Clark, R. A.; Rafailovich, M. H. Dual-syringe reactive electrospinning of cross-linked hyaluronic acid hydrogel nanofibers for tissue engineering applications. *Macromol. Biosci.* **2006**, *6* (10), 811−817.
(16) Vicini, S.; Mauri, M.; Vita, S.; Castellano, M. Alginate and alginate/hyaluronic acid membranes generated by electrospinning in wet conditions: Relationship between solution viscosity and spinnability. *J. Appl. Polym. Sci.* **2018**, *135* (25), No. 46390.
(17) Su, S.; Bedir, T.; Kalkandelen, C.; Ozan Başar, A.; Turkoğlu Şaşmazel, H.; Bulent Ustundag, C.; Sengor, M.; Gunduz, O. Coaxial and emulsion electrospinning of extracted hyaluronic acid and keratin based nanofibers for wound healing applications. *Eur. Polym. J.* **2021**, *142*, No. 110158.
(18) Ji, W.; Sun, Y.; Yang, F.; van den Beucken, J. J.; Fan, M.; Chen, Z.; Jansen, J. A. Bioactive electrospun scaffolds delivering growth factors and genes for tissue engineering applications. *Pharm. Res.* **2011**, *28* (6), 1259−1272.
(19) Wakuda, Y.; Nishimoto, S.; Suye, S.; Fujita, S. Native collagen hydrogel nanofibres with anisotropic structure using core-shell electrospinning. *Sci. Rep.* **2018**, *8* (1), 6248.
(20) Fujita, S.; Wakuda, Y.; Matsumura, M.; Suye, S. Geometrically customizable alginate hydrogel nanofibers for cell culture platforms. *J. Mater. Chem. B* **2019**, *7* (42), 6556−6563.
(21) Batnyam, O.; Shimizu, H.; Saito, K.; Ishida, T.; Suye, S.; Fujita, S. Biohybrid hematopoietic niche for expansion of hematopoietic stem/progenitor cells by using geometrically controlled fibrous layers. *RSC Adv.* **2015**, *5* (98), 80357−80364.
(22) Zhou, C.; Chu, R.; Wu, R.; Wu, Q. Electrospun polyethylene oxide/cellulose nanocrystal composite nanofibrous mats with homogeneous and heterogeneous microstructures. *Biomacromolecules* **2011**, *12* (7), 2617−2625.
(23) Deitzel, J. Controlled deposition of electrospun poly(ethylene oxide) fibers. *Polymer* **2001**, *42* (19), 8163−8170.
(24) Ponta, H.; Sherman, L.; Herrlich, P. A. CD44: from adhesion molecules to signalling regulators. *Nat. Rev. Mol. Cell Biol.* **2003**, *4* (1), 33−45.
(25) Cardoso, D. R.; Libardi, S. H.; Skibsted, L. H. Riboflavin as a photosensitizer. Effects on human health and food quality. *Food Funct.* **2012**, *3* (5), 487−502.
(26) Xue, F.; Zhang, H.; Hu, J.; Liu, Y. Hyaluronic acid nanofibers crosslinked with a nontoxic reagent. *Carbohydr. Polym.* **2021**, *259*, No. 117757.
(27) Ewaldz, E.; Brettmann, B. Molecular Interactions in Electrospinning: From Polymer Mixtures to Supramolecular Assemblies. *ACS Appl. Polym. Mater.* **2019**, *1* (3), 298−308.
(28) Brenner, E. K.; Schiffman, J. D.; Thompson, E. A.; Toth, L. J.; Schauer, C. L. Electrospinning of hyaluronic acid nanofibers from aqueous ammonium solutions. *Carbohydr. Polym.* **2012**, *87* (1), 926−929.
(29) Yao, S.; Wang, X.; Liu, X.; Wang, R.; Deng, C.; Cui, F. Effects of ambient relative humidity and solvent properties on the electrospinning of pure hyaluronic acid nanofibers. *J. Nanosci. Nanotechnol.* **2013**, *13* (7), 4752−4758.
(30) Li, J.; He, A.; Han, C. C.; Fang, D.; Hsiao, B. S.; Chu, B. Electrospinning of Hyaluronic Acid (HA) and HA/Gelatin Blends. *Macromol. Rapid Commun.* **2006**, *27* (2), 114−120.
(31) Liu, Y.; Ma, G.; Fang, D.; Xu, J.; Zhang, H.; Nie, J. Effects of solution properties and electric field on the electrospinning of hyaluronic acid. *Carbohydr. Polym.* **2011**, *83* (2), 1011−1015.
(32) Sun, J.; Perry, S. L.; Schiffman, J. D. Electrospinning Nanofibers from Chitosan/Hyaluronic Acid Complex Coacervates. *Biomacromolecules* **2019**, *20* (11), 4191−4198.
(33) Yamagata, M.; Uematsu, H.; Maeda, Y.; Suye, S.; Fujita, S. Bundling of Cellulose Nanofibers in PEO Matrix by Aqueous Electrospinning. *J. Fiber Sci. Technol.* **2021**, *77* (9), 223−230.
(34) Zhitong Shen; Suye, S.-i.; Fujita, S. In Situ Radical Polymerization of N-isopropylacrylamide in Electrospun Anisotropic Nanofiber of Poly (Ethylene Oxide). *J. Fiber Sci. Technol.* **2021**, *77* (1), 40−45.

https://doi.org/10.1021/acsomega.4c05851
ACS Omega 2024, 9, 40010−40018

(35) Vitkova, L.; Musilova, L.; Achbergerova, E.; Minarik, A.; Smolka, P.; Wrzecionko, E.; Mracek, A. Electrospinning of Hyaluronan Using Polymer Coelectrospinning and Intermediate Solvent. *Polymers* **2019**, *11* (9), 1517.
(36) Chen, H.; Chen, X.; Chen, H.; Liu, X.; Li, J.; Luo, J.; He, A.; Han, C. C.; Liu, Y.; Xu, S. Molecular Interaction, Chain Conformation, and Rheological Modification during Electrospinning of Hyaluronic Acid Aqueous Solution. *Membranes* **2020**, *10* (9), 217.
(37) Kayitmazer, A. B.; Koksal, A. F.; Kilic Iyilik, E. Complex coacervation of hyaluronic acid and chitosan: effects of pH, ionic strength, charge density, chain length and the charge ratio. *Soft Matter* **2015**, *11* (44), 8605−8612.
(38) Tiwari, S. K.; Venkatraman, S. S. Importance of viscosity parameters in electrospinning: Of monolithic and core−shell fibers. *Mater. Sci. Eng., C* **2012**, *32* (5), 1037−42.
(39) Ahire, J. J.; Robertson, D. D.; van Reenen, A. J.; Dicks, L. M. T. Polyethylene oxide (PEO)-hyaluronic acid (HA) nanofibers with kanamycin inhibits the growth of Listeria monocytogenes. *Biomedicine & Pharmacotherapy* **2017**, *86*, 143−148.
(40) Ionescu, O. M.; Mignon, A.; Iacob, A. T.; Simionescu, N.; Confederat, L. G.; Tuchilus, C.; Profire, L. New hyaluronic acid/polyethylene oxide-based electrospun nanofibers: design, characterization and in vitro biological evaluation. *Polymers* **2021**, *13* (8), 1291.
(41) Caykara, T.; Demirci, S.; Eroğlu, M. S.; Güven, O. Poly (ethylene oxide) and its blends with sodium alginate. *Polymer* **2005**, *46* (24), 10750−10757.
(42) Szymańska, E.; Wojasiński, M.; Czarnomysy, R.; Dębowska, R.; Łopianiak, I.; Adasiewicz, K.; Ciach, T.; Winnicka, K. Chitosan-enriched solution blow spun poly (ethylene oxide) nanofibers with poly (dimethylsiloxane) hydrophobic outer layer for skin healing and regeneration. *Int. J. Mol. Sci.* **2022**, *23* (9), 5135.
(43) Bhattarai, N.; Edmondson, D.; Veiseh, O.; Matsen, F. A.; Zhang, M. Electrospun chitosan-based nanofibers and their cellular compatibility. *Biomaterials* **2005**, *26* (31), 6176−6184.
(44) Collins, M. N.; Birkinshaw, C. Hyaluronic acid solutions—A processing method for efficient chemical modification. *J. Appl. Polym. Sci.* **2013**, *130* (1), 145−152.
(45) Gatej, I.; Popa, M.; Rinaudo, M. Role of the pH on hyaluronan behavior in aqueous solution. *Biomacromolecules* **2005**, *6* (1), 61−67.
(46) Razzak, M. A.; Kim, M.; Kim, H. J.; Park, Y. C.; Chung, D. Deciphering the interactions of fish gelatine and hyaluronic acid in aqueous solutions. *Int. J. Biol. Macromol.* **2017**, *102*, 885−892.
(47) Turgeon, S. L.; Laneuville, S. I. Protein + polysaccharide coacervates and complexes: from scientific background to their application as functional ingredients in food products. *Modern Biopolymer Science*; Academic Press, 2009; pp 327−363. .
(48) Yan, X.; Yu, M.; Ramakrishna, S.; Russell, S. J.; Long, Y. Z. Advances in portable electrospinning devices for in situ delivery of personalized wound care. *Nanoscale* **2019**, *11* (41), 19166−19178.
(49) Dong, R. H.; Jia, Y. X.; Qin, C. C.; Zhan, L.; Yan, X.; Cui, L.; Zhou, Y.; Jiang, X.; Long, Y. Z. In situ deposition of a personalized nanofibrous dressing via a handy electrospinning device for skin wound care. *Nanoscale* **2016**, *8* (6), 3482−3488.
(50) Haik, J.; Kornhaber, R.; Blal, B.; Harats, M. The Feasibility of a Handheld Electrospinning Device for the Application of Nanofibrous Wound Dressings. *Adv. Wound Care* **2017**, *6* (5), 166−174.
(51) Xu, S.; Lu, T.; Yang, L.; Luo, S.; Wang, Z.; Ye, C. In situ cell electrospun using a portable handheld electrospinning apparatus for the repair of wound healing in rats. *Int. Wound J.* **2022**, *19* (7), 1693−1704.
(52) Mouthuy, P. A.; Groszkowski, L.; Ye, H. Performances of a portable electrospinning apparatus. *Biotechnol. Lett.* **2015**, *37* (5), 1107−1116.
(53) Chui, C. Y.; Mouthuy, P. A.; Ye, H. Direct electrospinning of poly(vinyl butyral) onto human dermal fibroblasts using a portable device. *Biotechnol. Lett.* **2018**, *40* (4), 737−744.
(54) Revia, R. A.; Wagner, B. A.; Zhang, M. A Portable Electrospinner for Nanofiber Synthesis and Its Application for Cosmetic Treatment of Alopecia. *Nanomaterials* **2019**, *9* (9), 1317.
(55) Xu, S. C.; Qin, C. C.; Yu, M.; Dong, R. H.; Yan, X.; Zhao, H.; Han, W. P.; Zhang, H. D.; Long, Y. Z. A battery-operated portable handheld electrospinning apparatus. *Nanoscale* **2015**, *7* (29), 12351−12355.
(56) Yue, Y.; Gong, X.; Jiao, W.; Li, Y.; Yin, X.; Si, Y.; Yu, J.; Ding, B. In-situ electrospinning of thymol-loaded polyurethane fibrous membranes for waterproof, breathable, and antibacterial wound dressing application. *J. Colloid Interface Sci.* **2021**, *592*, 310−318.
(57) Yan, X.; Yu, M.; Zhang, L. H.; Jia, X. S.; Li, J. T.; Duan, X. P.; Qin, C. C.; Dong, R. H.; Long, Y. Z. A portable electrospinning apparatus based on a small solar cell and a hand generator: design, performance and application. *Nanoscale* **2016**, *8* (1), 209−213.
(58) Yan, X.; Duan, X.-P.; Yu, S.-X.; Li, Y.-M.; Lv, X.; Li, J.-T.; Chen, H.-Y.; Ning, X.; Long, Y.-Z. Portable melt electrospinning apparatus without an extra electricity supply. *RSC Adv.* **2017**, *7* (53), 33132−33136.
(59) Zhao, Y. T.; Zhang, J.; Gao, Y.; Liu, X. F.; Liu, J. J.; Wang, X. X.; Xiang, H. F.; Long, Y. Z. Self-powered portable melt electrospinning for in situ wound dressing. *J. Nanobiotechnol.* **2020**, *18* (1), 111.

https://doi.org/10.1021/acsomega.4c05851
ACS Omega 2024, 9, 40010−40018